RSC Advances

PAPER

View Article Online
View Journal | View Issue

Cite this: *RSC Adv.*, 2014, **4**, 47625

Application of supported Mn(III), Fe(III) and Co(II) as heterogeneous, selective and highly reusable nano catalysts for synthesis of arylaminotetrazoles, and DFT studies of the products

Davood Habibi,*[a] Ali Reza Faraji,*[b] Davood Sheikh,[c] Masoome Sheikhi[d] and Samaneh Abedi[e]

Received 8th July 2014
Accepted 8th September 2014

DOI: 10.1039/c4ra06463a

www.rsc.org/advances

M@Si/Al (where M = Mn(III), Co(II) and Fe(III) supported on nanosized SiO_2/Al_2O_3) is applied as an efficient, highly reusable and heterogeneous catalyst for the regiospecific synthesis of 1-aryl-5-amino-1*H*-tetrazole in dimethylformamide (DMF) as a solvent. The arylaminotetrazoles were efficiently synthesized from the reaction of cyanamides and sodium azide in the presence of a catalytic amount of nano metal catalyst under thermal conditions. 1-Aryl-5-amino-1*H*-tetrazoles (**B** isomer) can be obtained from the arylcyanamides carrying electron releasing substituents on the aryl ring, while with electron withdrawing groups, 5-arylamino-1*H*-tetrazole (**A** isomer) will be obtained. The advantages of this method include high yields, relatively short reaction times, easy work-up, recovery and reusability of the catalyst and high TON of catalyst. The nano catalyst can be easily recovered and reused several times without considerable loss of activity. The quantum theoretical calculations for the synthesized components were performed by density functional theory (DFT) methods using the 6-31G basis set, geometry and thermodynamic parameters, frontier molecular orbitals (FMOs) as well as by using molecular electrostatic potentials (MEPs).

Introduction

Technologies based on catalytic processes are of utmost importance for producing chemicals that have medical, environmental or economic importance. Many catalysts or catalytic systems have been developed to achieve these goals.[1] Homogenous catalysts due to their numerous available catalytic sites have many advantages such as high reactivity and selectivity.[2] Despite their advantages, some of the homogenous catalytic processes have not been commercialized because of difficulties encountered when attempting to separate and reuse the expensive noble metals. Furthermore, some industrial problems such as corrosion and deposition on reactor walls are associated with these homogeneous catalysts.[3] These disadvantages are minimized if homogeneous complexes are immobilized on organic polymers or inorganic solid supports with excellent chemical and thermal stability and easy accessibility such as clay, zeolites, SiO_2, mixed oxides and mesoporous materials. Covalent binding provides strong bonds between the support and the active site and thus helps to reduce metal contamination in the desired product. In the last decade, the syntheses of metal nanoparticles (NPs) have been developed. These nanoparticles are claimed to provide greater selectivity and control in heterogeneous catalysis.[2]

In the synthesis of compounds, limitation of natural resources, reduction of waste, maximizing renewability, and the development of environmentally benign reagents are the next challenges for the chemical sciences. Tetrazoles are widely used as ligands, as stable surrogates for carboxylic acids in medicinal chemistry, as explosive and information recording systems and also as precursors to a variety of nitrogen-containing compounds.[4–7] Among tetrazoles, aminotetrazoles are very interesting compounds and have received considerable attention as a result of their biological activity and interest to medicinal chemistry.[3,8] However, the lack of convenient methods for the preparation of arylaminotetrazoles strongly restricts their potential application in medical practice. Although many 5-substituted tetrazoles are known, only a few

[a]*Department of Organic Chemistry, Faculty of Chemistry, Bu-Ali Sina University, Hamedan 6517838683, Iran. E-mail: davood.habibi@gmail.com; Fax: +98 81 38380709; Tel: +98 81 38380922*

[b]*Young Researchers & Elite Club, Pharmaceutical Sciences Branch, Islamic Azad University, Tehran, Iran. E-mail: alireza_ch57@yahoo.com; Fax: +98 21 2264 0051; Tel: +98 21 2264 0051*

[c]*Young Researchers & Elite Club, Hamedan Branch, Islamic Azad University, Hamedan, Iran*

[d]*Young Researchers & Elite Club, Gorgan Branch, Islamic Azad University, Gorgan, Iran*

[e]*Department of Chemistry, Pharmaceutical Sciences Branch, Islamic Azad University, Tehran, Iran*

arylaminotetrazoles have been described. Generally, arylaminotetrazoles are synthesized by the condensation reaction of cyanamides with hydrazoic acid,[10] HOAc[9] and $FeCl_3$–SiO_2 (ref. 11) which results in a mixture of isomers, 5-arylamino-1*H*-tetrazoles and 1-aryl-5-amino-1*H*-tetrazoles. Due to the wide range of biological application of aminotetrazoles, the discovery and introduction of milder, faster, eco-friendly conditions resulting in high yields whilst using inexpensive reagents are in great demand.

Several regiospecific syntheses of arylaminotetrazoles have been reported through the [3 + 2] cycloaddition of cyanamides using NaN_3 in the presence of catalysts such as $ZnCl_2$ (ref. 12), $AlCl_3$ (ref. 13) and Iranian natrolite zeolite.[14] $ZnCl_2$ and $AlCl_3$ are homogeneous catalysts which cannot be separated from the reaction mixture. Reusability of the natrolite zeolite is an advantage, but its lack of availability is a disadvantage. Thus, the development of a catalytic synthetic method for tetrazoles still remains an active research area.

Industry favors catalytic processes induced by heterogeneous catalysts over homogeneous processes in view of the ease of handling, simple work-up, and regenerability.[15] Among catalysts, the application of nano catalysts has received considerable attention in recent decades as effective heterogeneous catalysts for organic synthesis due to their unique physical, surface chemical and catalytic properties.[16,17]

Due to safety considerations, we must avoid methods which use expensive and homogeneous catalysts. Because of the interesting applications of aminotetrazoles and in continuation of our interest in the synthesis of nitrogen-containing compounds and our ongoing research in heterogeneous catalysis,[12,17] herein we report our results for the synthesis of arylaminotetrazoles using nano catalysts as efficient heterogeneous catalysts at the desired temperature (Scheme 1).

Results and discussion

The catalytic activity and selectivity of different nano catalysts for the synthesis of various arylaminotetrazoles were investigated by using 2-chlorophenylcyanamide as a model substrate. Initial studies were performed in order to optimize the reaction conditions for the synthesis of 5-(2-chlorophenyl)amino-1*H*-tetrazole (isomer **A**) with sodium azide in the presence of these nano catalysts. To optimize the reaction conditions for syntheses of 5-(2-chlorophenyl)amino-1*H*-tetrazole in the presence of nano catalysts, various parameters such as the amount of the nano catalyst, the temperature, and the nature of the solvent, were investigated for their effect on the performance of the heterogeneous catalyst.

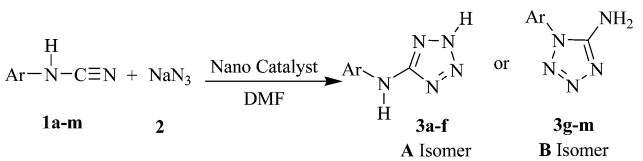

Scheme 1 Synthesis of arylaminotetrazoles using nano catalyst.

Table 1 Synthesis of arylaminotetrazoles catalyzed by various nano catalysts[a]

Entry	Catalyst (mg)	T (°C)	t (min)	Yield (%)	TON[b]	TOF[c]
1	Blank	100	180	—	—	—
2	Co(II)@Si/Al (200)	100	100	82	42.15	0.4215
3	Fe(III)@Si/Al (200)	100	100	64	4.671	0.0467
4	Fe(III)@Si/Al (200)	120	100	83	6.058	0.0605
5	Mn(III)@Si/Al (200)	100	100	79	22.57	0.2257
6	Co(II)@Si/Al (150)	100	100	83	57.34	0.5734
7	Fe(III)@Si/Al (150)	100	100	54	5.255	0.0525
8	Fe(III)@Si/Al (150)	120	100	82	7.980	0.0798
9	Mn(III)@Si/Al (150)	100	100	78	31.23	0.3123
10	Co(II)@Si/Al (100)	100	80	82	84.97	1.062
11	Fe(III)@Si/Al (100)	100	60	51	7.445	0.1240
12	Fe(III)@Si/Al (100)	120	110	82	11.97	0.1088
13	Mn(III)@Si/Al (100)	100	110	62	35.42	0.3220

[a] Reaction conditions: cyanamide (2 mmol), NaN_3 (3 mmol), solvent (6 mL). [b] TON, turn over number, moles of substrate converted per mole of metal. [c] TOF, turn over frequencies.

Synthesis of arylaminotetrazoles catalyzed by various nanosized M@Si/Al

The engaged catalysts in this reaction were simple structural Schiff base ligands that have the same support but different metals, including Mn(III)@Si/Al, Fe(III)@Si/Al, and Co(II)@Si/Al mixed oxide. The results are summarized in Table 1. Selected transmission electron microscope images of the catalysts are shown in Fig. 1. It can be seen that the appearance and size of the nanoparticles of the different catalysts were similar, demonstrating that the particles of SiO_2–Al_2O_3 have good mechanical stability and that they have not been destroyed during the whole modification. However, the average particle size in reverse micro emulsion solution of the catalysts was around 30, 29 and 28 nm for Mn(III)@Si/Al, Fe(III)@Si/Al, and Co(II)@Si/Al, respectively. Because of the small nanoparticle size and ligand capping as an obstacle in agglomeration, the M@Si/Al could be used as suitable catalysts for preparation of arylaminotetrazoles.

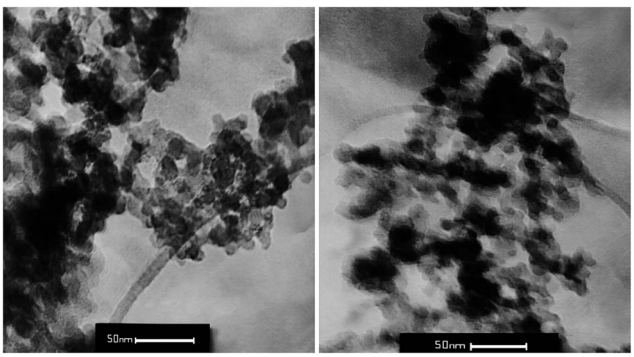

Fig. 1 TEM images corresponding to Mn@Si/Al sample (left) and Co@Si/Al (right).

The comparison of the capability and efficiency of Mn(III)@Si/Al, Fe(III)@Si/Al, and Co(II)@Si/Al together with the results of the application of these catalysts for the preparation of arylaminotetrazoles are presented in Table 1. As listed in Table 1, almost no reaction was observed in a blank experiment even though the reaction time was prolonged to 4 h at 120 °C. However, addition of the nano catalyst to the reaction mixture rapidly increased the synthesis of arylaminotetrazoles in high yields. The catalytic activity of these nano catalysts appeared to be dependent on the nature of the central ions. Co(II)@Si/Al presented the best activity among the three nano catalysts, and showed excellent catalytic performance under mild conditions. The different behavior and catalytic activities of the Co(II), Fe(III) and Mn(III) ions were probably influenced by the stability of the different valencies of the metal atoms and their electronic potentials.[18–21] As shown in Table 1, we calculated turn over numbers (TON) and turn over frequencies (TOF) as measures of the effectiveness of these catalysts in this reaction. The comparison TON (Co: 42.15, Fe: 4.671 and Mn: 22.57) and TOF (Co: 0.4215, Fe: 0.0467 and Mn: 0.2257) values of the nano catalysts indicated that the cobalt nano catalyst is more effective than the other nano catalysts. The catalytic activation of these catalysts was in the sequence Co(II)@Si/Al > Mn(III)@Si/Al > Fe(III)@Si/Al. The best result was obtained with the cyanamide–sodium azide ratio of 2 : 2.5 with 0.1 g of the nano Co catalyst at 100 °C (Table 1).

Effect of temperature on the synthesis of 5-(2-chlorophenyl) amino-1*H*-tetrazole

The effect of the reaction temperature on the synthesis of 5-(2-chlorophenyl) amino-1*H*-tetrazole catalyzed by the nano catalysts was investigated, and the results are summarized in Table 2. Increasing the temperature to accelerate the rate of reaction was apparently effective. Consequently, the effects of different temperatures (60 °C, 80 °C and 120 °C) were monitored for the synthesis of 5-(2-chlorophenyl)amino-1*H*-tetrazole after 100 min in the presence of the nano catalysts. Generally, by increasing the reaction temperature and time, the yields increased (>80%). Thus increasing the temperature was effective for the synthesis of 5-(2-chlorophenyl)amino-1*H*-tetrazole since at low temperature, the energy was not sufficient for the activation of the catalytic circulation.

Effect of solvent on the synthesis of 5-(2-chlorophenyl)amino-1*H*-tetrazole

In order to study the effects of solvents on the synthesis of 5-(2-chlorophenyl)amino-1*H*-tetrazole, acetonitrile, ethanol, water, benzene and dichloromethane were examined at 100 °C (Table 3). The reaction had low yields in the presence of coordinating solvents, while using water as a solvent caused no reaction to occur. It seems that the electron donor characteristics of these solvents caused them to occupy the vacant space around the metal in the catalysts, which prevented coordination from substrate molecules.[2,3] Therefore, water was not a suitable solvent for the synthesis of arylaminotetrazoles. Furthermore, not many organic solvents are stable at the high temperatures necessary for cycloaddition reactions and for this reason DMF is most commonly used for this purpose.[11,13–15]

Table 2 Effect of temperature on the synthesis of arylaminotetrazoles[a]

Entry	Catalyst	T (°C)	t (min)	Yield (%)
1	Co(II)@Si/Al	R.T	300	9
2	Co(II)@Si/Al	60	100	51
3	Co(II)@Si/Al	80	100	64
4	Co(II)@Si/Al	100	100	82
5	Co(II)@Si/Al	120	100	82
6	Fe(III)@Si/Al	R.T	100	8
7	Fe(III)@Si/Al	60	100	47
8	Fe(III)@Si/Al	80	100	60
9	Fe(III)@Si/Al	100	100	73
10	Fe(III)@Si/Al	120	100	82
11	Mn(III)@Si/Al	R.T	100	Trace
12	Mn(III)@Si/Al	60	100	32
13	Mn(III)@Si/Al	80	100	51
14	Mn(III)@Si/Al	100	100	79
15	Mn(III)@Si/Al	120	100	79

[a] Reaction conditions: cyanamide (2 mmol), NaN_3 (3 mmol), solvent (6 mL).

Synthesis of various arylaminotetrazoles catalyzed by nano catalysts

A series of phenylcyanamides were converted into the corresponding arylaminotetrazoles with sodium azide by the nano catalysts in high yields under the thermal conditions (Table 4). Phenylcyanamides containing both electron-donating and electron-withdrawing groups underwent the conversion in good yields.

As shown in Table 4, we evaluated the electronic effect of the substituents attached to the benzene ring in the cyanamides. The substrates having electron donating groups (EDGs) on the benzene rings (entries 7–9, 12 and 13) complete the reaction at 100 °C after 55 min, while species with electron-withdrawing groups (EWGs) (entries 1–4 and 6) require longer reaction times.

Table 3 Effect of solvent on the synthesis of arylaminotetrazoles[a]

Entry	Catalyst[b]	Solvent	t (min)	Yield[b] (%)
1	Co(II)@Si/Al	DMF	100	83
2	Fe(III)@Si/Al	DMF	110	83
3	Mn(III)@Si/Al	DMF	110	79
4	Co(II)@Si/Al	DMSO	300	72
5	Fe(III)@Si/Al	DMSO	300	70
6	Mn(III)@Si/Al	DMSO	300	65
7	Co(II)@Si/Al	H_2O	300	5
8	Fe(III)@Si/Al	H_2O	300	5
9	Mn(III)@Si/Al	H_2O	300	Trace

[a] Reaction conditions: cyanamide (2 mmol), NaN_3 (3 mmol), solvent (6 mL). [b] Isolated yield.

Table 4 Synthesis of arylaminotetrazoles using nano catalysts[a]

Entry	Substrate (1)	Product (3) (isomer A or B)	Catalyst[b]	Time (min)	Yield (%)	TON[c]	TOF[d]	Ref.
1	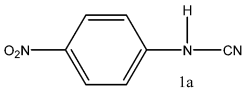 1a	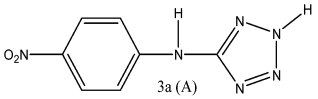 3a (A)	Co(II)@Si/Al	115	80	82.90	0.7201	
			Fe(III)@Si/Al	125	78	11.83	0.0910	11 and 12
			Mn(III)@Si/Al	130	82	31.24	0.2402	
2	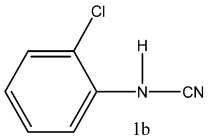 1b	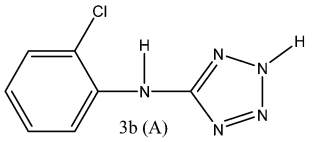 3b (A)	Co(II)@Si/Al	100	82	84.97	0.8498	
			Fe(III)@Si/Al	110	82	11.97	0.1088	11
			Mn(III)@Si/Al	125	83	31.62	0.2530	
3	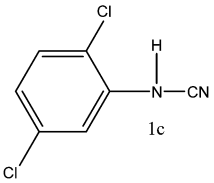 1c	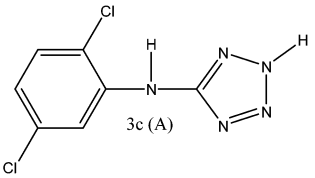 3c (A)	Co(II)@Si/Al	100	79	81.86	0.8187	
			Fe(III)@Si/Al	120	78	11.38	0.0948	12
			Mn(III)@Si/Al	130	80	30.48	0.2344	
4	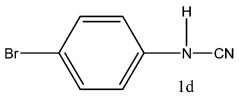 1d	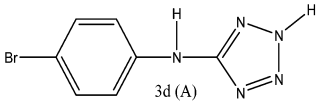 3d (A)	Co(II)@Si/Al	95	81	98.44	1.036	
			Fe(III)@Si/Al	115	79	10.65	0.0927	11–13
			Mn(III)@Si/Al	110	83	31.62	0.2874	
5[e]	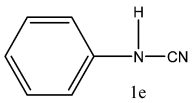 1e	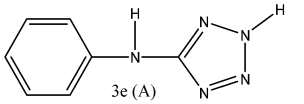 3e (A)	Co(II)@Si/Al	75	78	80.82	0.8508	
			Fe(III)@Si/Al	85	75	10.95	0.1288	—
			Mn(III)@Si/Al	100	80	30.48	0.3048	
6	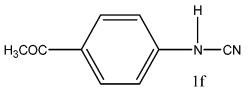 1f	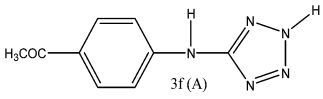 3f (A)	Co(II)@Si/Al	110	80	82.90	0.7536	
			Fe(III)@Si/Al	110	78	11.37	0.1035	12
			Mn(III)@Si/Al	120	80	30.48	0.2540	
7	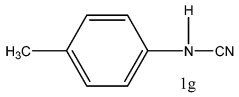 1g	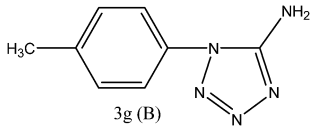 3g (B)	Co(II)@Si/Al	55	83	86.01	1.433	
			Fe(III)@Si/Al	90	83	12.12	0.1346	11–13
			Mn(III)@Si/Al	75	82	31.24	0.4165	
8	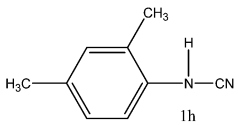 1h	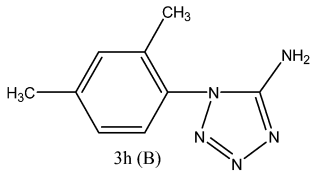 3h (B)	Co(II)@Si/Al	55	79	81.86	1.488	
			Fe(III)@Si/Al	85	76	11.090	0.1305	11–13
			Mn(III)@Si/Al	70	75	28.57	0.4082	
9	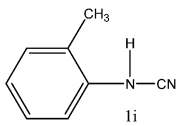 1i	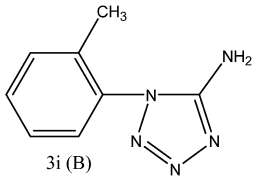 3i (B)	Co(II)@Si/Al	55	80	82.90	1.275	
			Fe(III)@Si/Al	65	80	11.68	0.1800	13
			Mn(III)@Si/Al	70	81	30.86	0.4408	
10	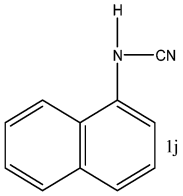 1j	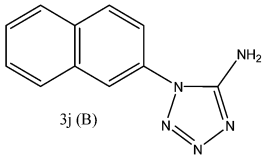 3j (B)	Co(II)@Si/Al	55	81	83.94	1.526	
			Fe(III)@Si/Al	85	82	11.97	0.1408	11 and 13
			Mn(III)@Si/Al	65	79	30.10	0.4630	
11	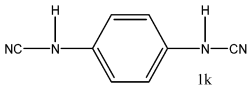 1k	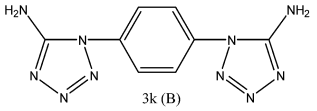 3k (B)	Co(II)@Si/Al	30	83	86.01	1.075	
			Fe(III)@Si/Al	130	74	10.80	0.0831	12
			Cat.3	110	80	30.48	0.2770	

Table 4 (*Contd.*)

Entry	Substrate (**1**)	Product (**3**) (isomer **A** or **B**)	Catalyst[b]	Time (min)	Yield (%)	TON[c]	TOF[d]	Ref.
12	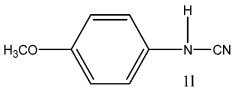 1l	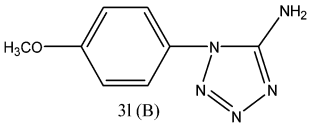 3l (B)	Co(II)@Si/Al Fe(III)@Si/Al Mn(III)@Si/Al	55 80 80	78 72 80	80.82 10.51 30.48	1.616 0.1314 0.3810	11–13
13[e]	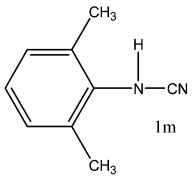 1m	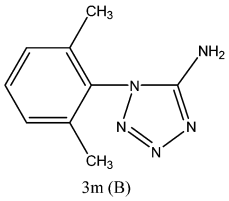 3m (B)	Co(II)@Si/Al Fe(III)@Si/Al Mn(III)@Si/Al	55 80 65	78 74 76	80.82 10.80 28.95	1.469 0.1350 0.4454	—

[a] Reaction conditions: cyanamide (2 mmol), NaN_3 (3 mmol), solvent (6 mL). [b] Co(II)@Si/Al (100 mg); Fe(III)@Si/Al (100 mg); Mn(III)@Si/Al (150 mg). [c] TON, turn over number, moles of substrate converted per mole of metal. [d] TOF, turn over frequencies. [e] Analytical data (m.p., ^{1}H NMR, ^{13}C NMR and elemental analysis) for selected compound.

Also, the arylaminotetrazoles were completely regiospecific. In most cases, in the synthesis of arylaminotetrazoles from cyanamides, only the 1-aryl-5-amino-1*H*-tetrazole (**B**) or a mixture of isomers (**A** + **B**) was obtained[10] and the nature of the substituent did not have any effect.[22–26] Previously, Garbrecht and coworkers showed that different substituents (such as the *p*-methyl and the *p*-nitrophenyl group) permit the formation of the same type of compound (isomer **B**).[9] However, in our methods, arylaminotetrazole derivatives (**3**) are strongly affected by the type of substituents in the phenylcyanamides (**1**) which determine the obtained isomers 1-aryl-5-amino-1*H*-tetrazoles (**B**) or 5-arylamino-1*H*-tetrazoles (**A**) (Table 4). Generally, when the substituent on the aryl ring of **1** is an EDG, formation of 1-aryl-5-amino-1*H*-tetrazoles (**B**) is favored (entries 7–9, 12 and 13, Table 4), and as the electronegativity of the substituent is increased, the product is shifted toward 5-arylamino-1*H*-tetrazoles (**A**) (entries 1–4 and 6, Table 4). This observation correlates with results obtained from the synthesis of arylaminotetrazoles using $ZnCl_2$, $AlCl_3$ or natrolite zeolite.[12,13]

4-Nitrophenylcyanamide (Table 4, entry 1) interestingly gave 5-(4-nitrophenyl) amino-1*H*-tetrazole (**A** isomer), while with HN_3, AcOH and $FeCl_3$–SiO_2, 1-(4-nitrophenyl)-5-amino-1*H*-tetrazole (**B** isomer) or the mixture of isomers (**A** + **B**) were obtained.[8–10] Interestingly **1k** afforded the double-addition product in 83% isolated yield (Table 4, entry 11).

Proposed mechanism

The nano catalyst probably has an important role in the promotion of the synthesis of arylaminotetrazoles as a Lewis acid and the plausible mechanism is shown in Scheme 2. To further elucidate the reaction mechanism, a series of experiments was conducted. When the synthesis of arylaminotetrazoles was conducted in the absence of nano catalyst, the yield of reaction could only reach 5%. However, the yields were remarkably increased by adding nano catalyst to the mixture (Table 4, 82%, entry 2). The results indicate that the nano catalyst is crucial for this reaction. According to the proposed mechanism, the nano catalyst may show complexation towards the nitrile group of cyanamides and thus may enhance the electrophilic character. It involves activation of the nitrile group over the surface of the nano catalyst and subsequent nucleophilic attack of the sodium azide.[12–15] The results indicated that the process was completely regiospecific. There is an excellent correlation between the type of different substitution on the aryl ring and the major product. Indeed, when the substitution on the benzene ring is electron-donating in arylcyanamides (Table 4, entries 7–13), the formation of 1-aryl-5-amino-1*H*-tetrazoles (**B**) is favored *via* a guanidine azide intermediate (II) and as the electronegativity of the substituent is increased (Table 4, entries 1–6), the type of product is changed to 5-arylamino-1*H*-tetrazole (**A**). In other words, if cyclization [3 + 2] were to involve the nitrogen carrying the aryl substituent in the guanidine azide intermediate (II), 1-aryl-5-amino-1*H*-tetrazoles would result.

In addition, our results indicated that the nature of the substituent plays a minor role in directing the course of the reaction when the reaction is carried out for 24 h at 120 °C. In

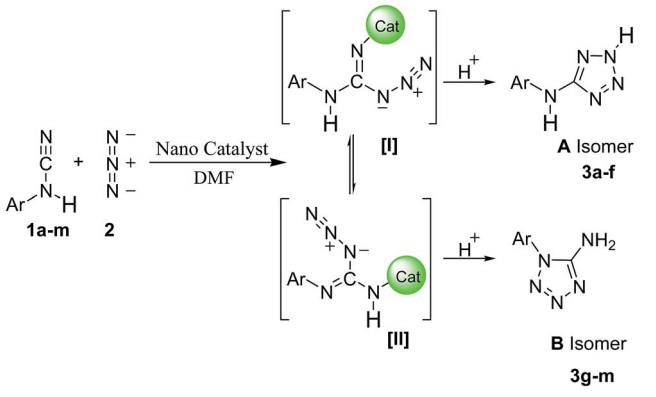

Scheme 2 Mechanism of nano metal catalyzed synthesis of arylaminotetrazoles.

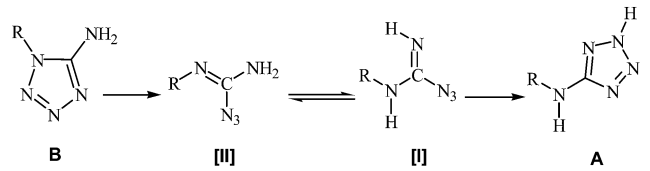

Scheme 3 Transformation of isomer B to isomer A in harsh conditions.

Table 5 Dipole moment (μ), ΔE and point group of molecules **3a–3m** obtained using B3LYP/6-31G level

Substrate	μ (Debye)	ΔE (Hartree Fock)	Point group
3a	5.2294	−748.9052	C_1
3b	3.7543	−1004.0463	C_1
3c	2.0515	−1463.6192	C_1
3d	1.2847	−3115.4547	C_1
3e	1.6960	−544.4830	C_1
3f	2.1027	−697.0849	C_1
3g	7.9860	−583.7897	C_1
3h	7.8898	−623.0982	C_1
3i	7.3901	−583.7893	C_1
3j	7.5465	−698.0883	C_1
3k	6.2357	−856.7596	C_1
3l	7.7578	−658.9646	C_1
3m	7.3499	−623.0978	C_1

these conditions, substituents which differ in their electrical effects (such as methyl or *p*-methoxy group) permit the formation of compound (**A**) as a stable product in high yield (>95%), presumably through the intermediate formation of a guanyl azide (Scheme 3).

Theoretical calculations

We have carried out quantum theoretical calculations of tetrazole derivatives using the B3LYP/6-31G level (DFT) by the Gaussian 03 software package.[27] Some electronic properties such as energy of the highest occupied molecular orbital (E_{HOMO}), energy of the lowest unoccupied molecular orbital (E_{LUMO}), energy gap (ΔE) between LUMO and HOMO, atomic charges, dipole moment (μ) and point group were determined. The optimized molecular structures and HOMO and LUMO surfaces were visualized using the GaussView 03 program.[28] We also studied the thermodynamic parameters of molecules **3a–3m** using the B3LYP/6-31G level, and obtained the energy (ΔE), enthalpies (ΔH), Gibbs free energy (ΔG), entropies (S) and constant volume molar heat capacity (C_v) of the derivatives.[29]

The optimized geometrical parameters, such as dipole moment (μ; Debye), energy of structure formation (ΔE; Hartree Fock) and point group, using the B3LYP/6-31G level are listed in Table 5. According to Table 5, the geometry of the structures under investigation is C_1 point group symmetry.

Dipole moment (μ) is a good measure for the asymmetry of a molecule. The values listed in Table 5 show that among molecules **3a–3m**, the largest value of dipole moment is obtained for molecule **3g** and the smallest value is obtained for molecule **3d**. According to Table 5, energy of structure formation (ΔE) for molecule **3d** is more negative, therefore product **3d** has the most stable structure. Product **3e** has the most unstable structure.

Frequency calculations

The relative energy (ΔE), standard enthalpies (ΔH), entropies (ΔS), Gibbs free energy (ΔG) and constant volume molar heat capacity (C_v) values of derivatives **3a–3m** were obtained by theoretical methods using the B3LYP/6-31G level to obtain minima of the potential energy. The calculated results in Table 6 show that relative energy, Gibbs free energy and standard enthalpy values of all molecules are negative, therefore we found that all molecules are stable. As indicated in Table 6, and according to the previous section, we found that the product **3d** has maximum stability because it has the greatest amount of relative energy (ΔE), Gibbs free energy (ΔG) and standard enthalpy (ΔH) whereas the product **3e** has the most instability because it has the smallest values of ΔE, ΔG and ΔH. The

Table 6 The calculated thermodynamic parameters of molecules **3a–3m** using the B3LYP/6-31G level

Substrate	ΔE (kcal mol^{-1})	ΔG (kcal mol^{-1})	ΔH (kcal mol^{-1})	S (cal/molK)	C_V (cal/molK)
3a	−469 851.856	−469 876.359	−469 844.142	108.056	43.132
3b	−629 963.214	−629 986.918	−629 956.142	103.221	38.881
3c	−918 355.754	−918 380.791	−918 347.883	110.375	42.845
3d	−1 954 891.651	−1 954 915.709	−1 954 884.588	104.378	38.671
3e	−341 576.225	−341 598.276	−341 570.073	94.595	34.566
3f	−437 311.693	−437 336.832	−437 303.344	112.321	46.772
3g	−366 225.235	−366 249.287	−366 217.668	106.050	42.177
3h	−390 874.303	−390 899.897	−390 865.585	115.083	48.219
3i	−366 224.904	−366 248.398	−366 217.407	103.942	42.165
3j	−437 936.322	−437 960.587	−437 928.325	108.208	47.669
3k	−537 506.888	−537 533.666	−537 497.290	122.005	55.727
3l	−413 395.218	−413 419.509	−413 387.157	108.511	45.595
3m	−390 873.897	−390 898.926	−390 865.297	112.794	48.110

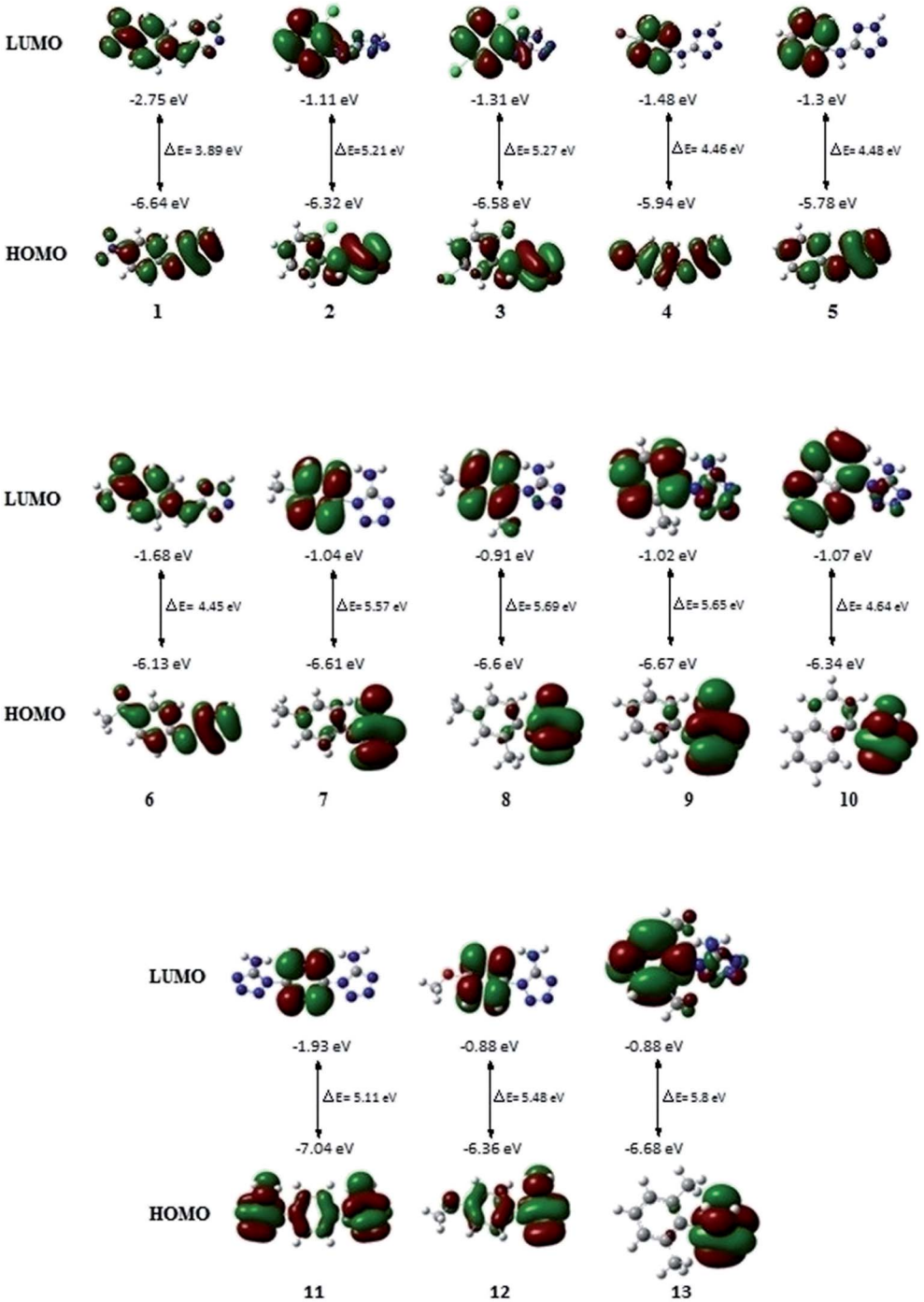

Fig. 2 Frontier molecular orbitals of compounds **3a–3m**. (Δ*E*: energy gap between LUMO and HOMO).

entropies (Δ*S*) and constant volume molar heat capacity (C_v) values do not seem to follow a similar trend.

Frontier molecular orbital analysis

The E_{HOMO}, E_{LUMO} and HOMO–LUMO energy gap of molecules **3a–3m** were calculated using the B3LYP/6-31G level. Molecular orbitals and their properties, such as energy and frontier electron density, are important and are used to determine the reactive position in π-electron systems.[30] Therewith, values of energy of the lowest unoccupied molecular orbital (LUMO) and the highest occupied molecular orbital (HOMO) and their energy gaps reflect the chemical activity of the molecules.[31] According to HOMO and LUMO orbital pictures (Fig. 2), it is found that the filled π-orbital (HOMO) is mostly located on the tetrazole ring of the compounds, while the unfilled anti π-orbital (LUMO) is on the benzene ring. When electron transitions take place, electrons are mainly transferred from the tetrazole ring to the phenyl ring. The HOMO can act as an electron

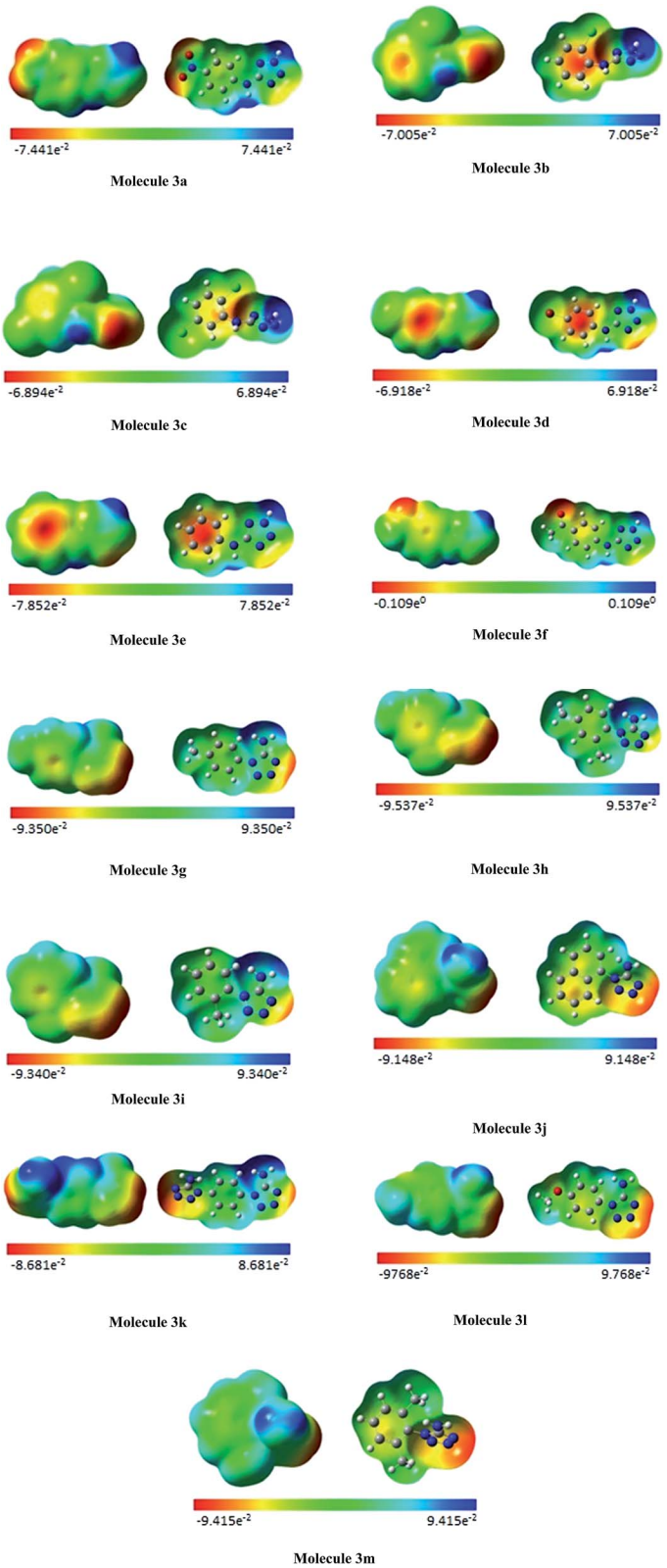

Fig. 3 The molecular electrostatic potential surface of molecules **3a–3m**.

donor and the LUMO can act as the electron acceptor. A higher HOMO energy (E_{HOMO}) for the molecule indicates a higher electron-donating ability to an appropriate acceptor molecule with a low-energy empty molecular orbital. As shown in Fig. 2, the HOMO energy of compound **3e** has the highest value (−5.78 eV). In addition, a large energy gap implies high stability for the

molecule. Fig. 2 shows that the energy gap of compound **3m** has the highest value (5.8 eV) therefore it is less reactive than other structures. Also the energy gap of structure **3a** has the lowest value (3.89 eV), which indicates that it is more reactive. It implies that the electronic transfer in molecule **3a** is easier. The existence of the electron withdrawing nitro group ($-NO_2$) in molecule **3a** reduces the energy of the HOMO.

Molecular electrostatic potential

Molecular electrostatic potential (MEP) is related to the electronic density and is important in understanding sites for electrophilic attack and nucleophilic reactions.[32–34] MEP is a graphic model and a real physical property.[35] This methodology is used to investigate the electronic distribution in molecules and to evaluate the electronic distribution around molecular surfaces for compounds.[36,37]

To indicate the sites on the molecules for interaction with electrophilic and nucleophilic species, MEP was calculated at the B3LYP/6-31G optimized geometry for structures **3a–3m**. As shown in both Fig. 3 and 4, electrophilic reactivities are red in color which indicates the negative regions of the molecule, while the nucleophilic reactivities are colored in blue and indicate the positive regions of the molecule. The nitro and carbonyl oxygen atoms are surrounded by a greater negative charge surface, making these sites potentially more favorable for electrophilic attack. According to Fig. 3 and 4, in the MEP of molecules **3a–3m**, negative centers include the tetrazole ring, phenyl ring and oxygen atoms (red color). Among the MEPs of molecules **3a–3f**, the MEPs of molecules **3a** and **3e** indicate that their phenyl ring and oxygen atom have higher electronic density than other molecules (Fig. 3). Also, it can be seen from Fig. 3, that the main negative center is focused on the tetrazole ring. Among molecules **3g–3m**, molecule **3l** has the greatest electronic density on the tetrazole ring (Fig. 3).

The electronic density of the atoms of derivatives **3a–3m** is shown in Fig. 4. The negative charges are mainly located on N atoms, C phenyl ring atoms and O atoms. All H atoms are positive. According to Fig. 4, the highest negative charge in molecules **3a–3f** focused on an N atom attached to the phenyl ring (N–H) while the highest negative charge in molecules **3g–3m** is focused on N (N–H_2) on the tetrazole ring (attached to the phenyl ring).

Catalyst reuse and stability

In order to examine the leaching of metal (Mn and Co) from the heterogeneous catalyst, a series of experiments was conducted in which the nano catalyst was filtrated after 20, 30 and 60 min and the reactions were continued with the filtrate. For this purpose, the reaction of 5-(2-chlorophenyl) amino-1*H*-tetrazole with sodium azide in the presence of nano catalyst in DMF solvent was studied. After 20 min (the reaction normally completed within 100 min with 82% yield of product), the reaction was stopped and catalyst was removed by filtration from the reaction mixture. Then the mixture without the solid catalyst which contains unreacted substrates was allowed to continue under the same conditions. In these conditions the reaction did not proceed at all; the data indicated that the leaching of metal from the solid support was low. For practical applications of heterogeneous catalysts, the reusability is a very

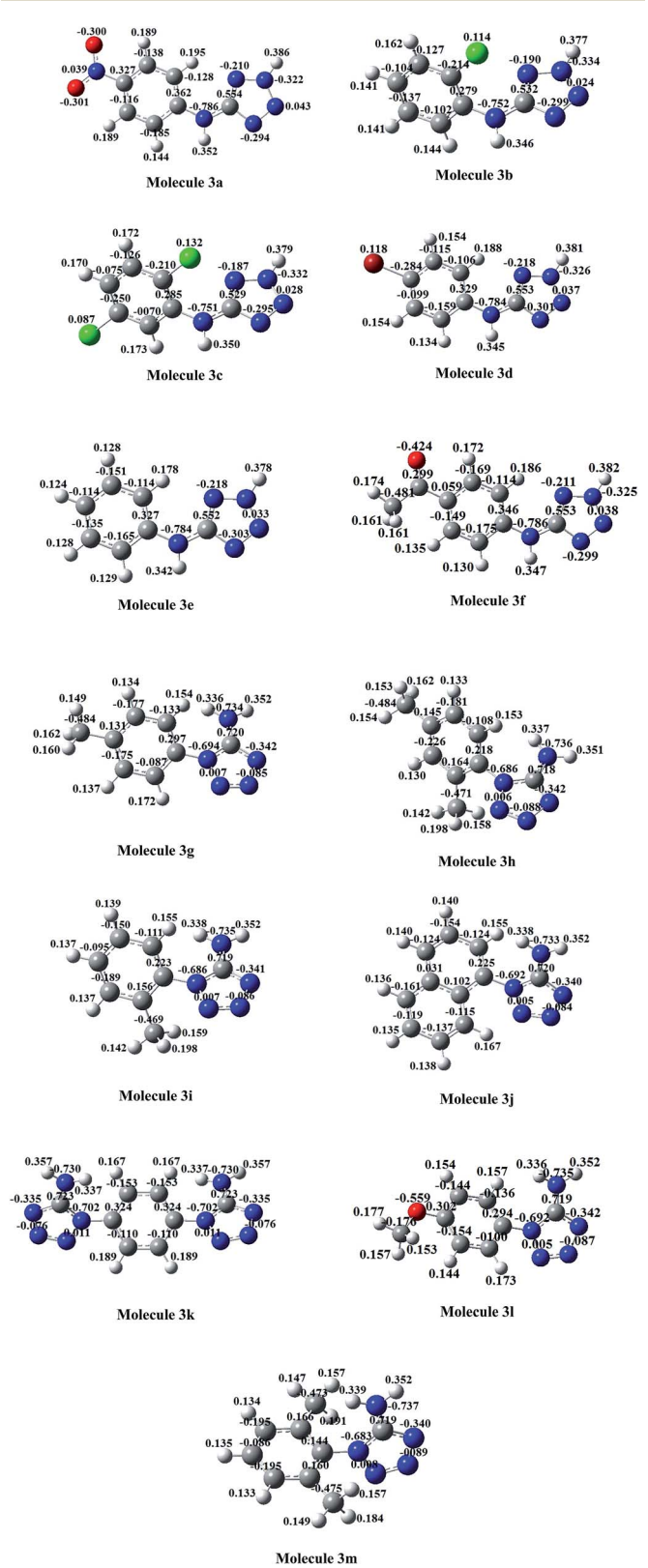

Fig. 4 Electronic density of the atoms of structures **3a–3m**.

significant factor. The reusability of the catalysts was checked in the reaction of 4-methylphenylcyanamide with sodium azide as the substrates under the present reaction conditions (Table 1, entry 2). After completion of the reaction in the first run, the catalyst was separated from the reaction mixture by a simple filtration and the resulting solid mass was reused for the next run. In the case of the cobalt nano catalyst the recovered catalyst activities of five consecutive runs were about 83%, 82%, 81%, 81% and 80% respectively. This demonstrates the practical recyclability of this catalyst. Furthermore, in the case of Mn(III)@Si/Al and Fe(III)@Si/Al, the nano catalysts have been recovered for 7 runs with some decrease in the catalytic activity of the catalyst.

Experimental

All reagents were purchased from the Merck and Aldrich chemical companies and used without further purification. All compounds were characterized by different spectroscopic methods (IR, FT-IR, ^{1}H NMR and ^{13}C NMR), elemental analysis (CHN) and melting points and identified by comparison of their physical and spectroscopic data with those of authentic samples. The NMR spectra were recorded in acetone, DMSO and $CDCl_3$. ^{1}H NMR spectra were recorded on Bruker Avance DRX 100, 300 and 500 MHz instruments. The chemical shifts (δ) are reported in ppm relative to the TMS as internal standard. J values are given in Hz. IR (KBr) spectra were recorded on a Shimadzu 470 and Perkin-Elmer 781 spectrophotometer. Melting points were taken in open capillary tubes with a BUCHI 510 melting point apparatus and were uncorrected. The elemental analysis was performed using a Heraeus CHN-O-Rapid analyzer. Thin layer chromatography (TLC) was performed on silica gel polygram SIL G/UV 254 plates.

Preparation of nanosized organometallic-SiO_2/Al_2O_3

Nanosized SiO_2/Al_2O_3 was used as the support and prepared by the sol–gel method.[18,19] At first, 3.5 g nanosized SiO_2/Al_2O_3 was activated at 500 °C for 5 h under air and then was refluxed with 4.3 mL of trimethoxysilylpropylamine (3-APTMS) in dry toluene (50 mL) for 24 h. The solid achieved during this process was filtered and washed off with dry methanol at 100 °C under vacuum for 5 h. Then bipyridylketone (BPK) was added to a suspended solution of the Si/Al–APTMS in dry methanol. To synthesize Si/Al–APTMS–BPK–Co(II) and Si/Al–APTMS–BPK–Mn(III), 2.0 g Si/Al–APTMS–BPK was suspended in 50 mL of ethanol in a round bottom flask followed by addition of 3.0 mmol $Co(OAc)_2\cdot 4H_2O$ and $Mn(OAc)_2\cdot 4H_2O$, respectively. The mixture was refluxed during 24 h under magnetic stirring. Furthermore, to synthesize Si/Al–APTMS = ferrocene, the ferrocenecarboxaldehyde (FCA) was added to a suspended solution of Si/Al supported aminopropyl (Si/Al–APTMS) in dry methanol.

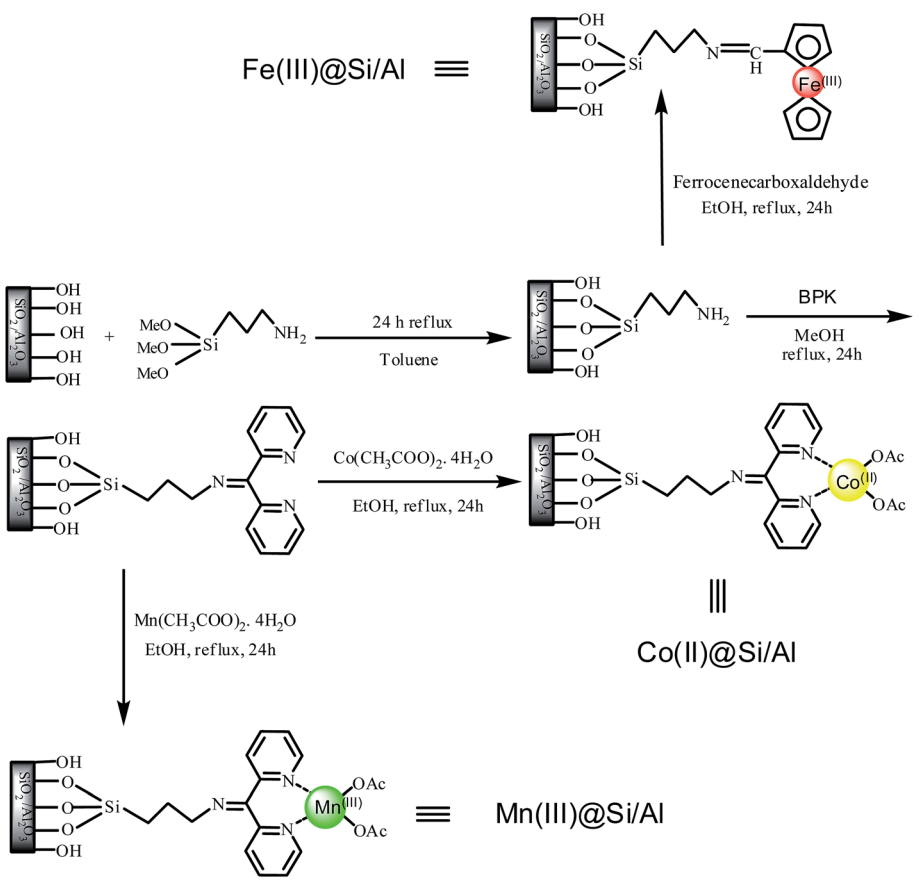

Scheme 4 Schematic representation of the preparation process for nano catalysts.

The mixture was refluxed for 24 h to make a Fe nano catalyst on the surface of nano scale Si/Al (Scheme 4). The formation of nano catalyst on the SiO_2/Al_2O_3 mixed oxides was verified using BET, elemental analysis, FT-IR, UV-vis, BET, ICP, SEM, EDS, XPS, TGA and TEM.[2,3,18,19]

General procedure for the synthesis of arylaminotetrazoles using the nano catalyst

The nano catalyst was added to a mixture of cyanamides (**1a–m**) (2 mmol), sodium azide (200 mg, 3 mmol) and distilled dimethylformamide (6 mL) and stirred at the desired temperature for the appropriate time (Table 4). After completion of the reaction (as monitored by TLC), the catalyst was centrifuged, washed with ethyl acetate and the centrifugate was treated with EtOAc (3 × 10 mL) and 5 N HCl (20 mL) and stirred vigorously. The resultant organic layer was separated and the aqueous layer was again extracted with ethyl acetate (25 mL). The combined organic layers were washed with water, the solvent removed and the crude solid arylaminotetrazole recrystallized (aqueous ethanol). The pure products were characterized by IR and NMR. The physical data (mp, IR, ^{1}H NMR, ^{13}C NMR) of known compounds were found to be identical with those reported in the literature.[11–14]

Analytical data for selected compounds

5-(4-Acethylphenyl)amino-1*H*-tetrazole (1e, Table 4, entry 6). M.p.: 215–217°C; ^{1}H NMR (300 MHz, DMSO-d_6): 10.38 (s, 1H), 7.92 (d, J = 7.95 Hz, 2H), 7.14 (d, J = 7.64 Hz, 1H), 1.10 (s, 1H) ppm; ^{13}C NMR (75 MHz, DMSO-d_6): 196.7, 145.3, 130.4, 130.1, 116.2, 31.7, 26.8; IR (KBr): $\bar{\nu}$ = 3403, 3282, 3177, 3024, 2978, 2839, 2780, 2440, 1651, 1627, 1605, 14 579, 1470, 1426, 1364, 1285, 1258, 1195, 1055, 1024, 962, 885, 865, 835, 733, 592 cm^{-1}; anal. calcd for $C_9H_5N_5O$: C, 53.20; H, 4.46; N, 34.47. Found: C, 53.16; H, 4.39; N, 35.12%.

1-(2,6-Dimethylphenyl)-5-amino-1*H*-tetrazole (1m, Table 4, entry 13). M.p. 148–149°C; ^{1}H NMR (500 MHz, DMSO-d_6): 7.02 (s, 3H), 5.19 (s, 2H), 2.27 (s, 6H) ppm; ^{13}C NMR (125 MHz, DMSO-d_6): 157.5, 137.6, 136.6, 128.3, 126.3, 18.5 ppm; IR (KBr): $\bar{\nu}$ = 3430, 3295, 3070, 2955, 2920, 2854, 1654, 1600, 1579, 1535, 1477, 1440, 1376, 1349, 1260, 1217, 1160, 1114, 917, 869, 760, 700, 662, 636, 546, 516, 496 cm^{-1}; anal. calcd for $C_9H_{11}N_5$: C, 57.12; H, 5.86; N, 37.02. Found: C, 57.45; H, 5.67; N, 36.57%.

Conclusions

In conclusion, a simple and convenient method has been developed for the synthesis of arylaminotetrazoles in the presence of the nano catalyst as a heterogeneous reusable catalyst under thermal conditions. Well-dispersed Fe, Mn and Co nanoparticles have been prepared on a SiO_2/Al_2O_3 nanosized heterogeneous support and have been successfully employed and tested in the syntheses of arylaminotetrazoles. The significant advantages of this methodology are high yields, mild reaction conditions, elimination of dangerous and harmful hydrazoic acid and a simple work-up procedure. The nano catalyst can be recovered and reused by simple filtration with a tiny decrease in activity. The proposed methodology could be used in organic synthesis for the syntheses of arylaminotetrazoles.

In the present work, we have performed theoretical analyses of tetrazole derivatives by density functional theory calculations using the B3LYP/6-31G level. The thermodynamic parameters, frontier molecular orbitals (HOMO and LUMO), and electronic density (MEP) were obtained. Based on the thermodynamic parameters we found that all molecules are stable. The presence of the nitro group (NO_2) in molecule **3a** reduces the energy of the HOMO, therefore the HOMO–LUMO energy gap of molecule **3a** is the smallest (3.89 eV). The other molecular properties such as dipole moment (μ), energy of structure formation (ΔE; Hartree Fock) and point group were calculated. As shown by the MEPs, among molecules **3a–3f**, molecules **3b** and **3c** have the greatest electronic density on the tetrazole ring and among **3g–3m**, molecule **3l** has the greatest electronic density on the tetrazole ring.

Acknowledgements

We thank the research council of Bu-Ali Sina and the Islamic Azad University for financial support.

Notes and references

1 R. J. Herr, *Bioorg. Med. Chem.*, 2002, **10**, 3379.
2 D. Habibi, A. R. Faraji, M. Arshadi and J. L. G. Fierroc, *J. Mol. Catal. A: Chem.*, 2013, **372**, 90; M. Uyanik, M. Akakura and K. Ishihara, *J. Am. Chem. Soc.*, 2009, **131**, 251.
3 D. Habibi and A. R. Faraji, *C. R. Chim.*, 2013, **16**, 888; M. Uyanik and K. Ishihara, *Chem. Commun.*, 2009, 2086; B. Zeynizadeh and P. Lotfi, *Asian J. Chem.*, 2009, **21**, 3617.
4 G. F. Holland and J. N. Pereira, *J. Med. Chem.*, 1967, **10**, 149.
5 L. A. Flippin, *Tetrahedron Lett.*, 1991, **32**, 6857.
6 P. Rhonnstad and D. Wensbo, *Tetrahedron Lett.*, 2002, **43**, 3137.
7 E. O. John, R. L. Kirchmeier and J. M. Shreeve, *Inorg. Chem.*, 1989, **28**, 4629.
8 N. P. Peet, L. E. Baugh, S. Sundler, J. E. Lewis, E. H. Matthews, E. L. Olberding and D. N. Shah, *J. Med. Chem.*, 1968, **29**, 2403.
9 W. L. Garbrecht and R. M. Herbst, *J. Org. Chem.*, 1953, **18**, 1014.
10 A. R. Modarresi-Alam and M. Nasrollahzadeh, *Turk. J. Chem.*, 2009, **33**, 267.
11 D. Habibi and M. Nasrollahzadeh, *Synth. Commun.*, 2010, **40**, 3159.
12 M. Nasrollahzadeh, D. Habibi, A. R. Faraji and Y. Bayat, *Tetrahedron*, 2010, **66**, 3866.
13 D. Habibi, M. Nasrollahzadeh and Y. Bayat, *Synth. Commun.*, 2011, **41**, 2135.
14 M. Nasrollahzadeh, D. Habibi, Z. Shahkarami and Y. Bayat, *Tetrahedron*, 2009, **65**, 10715.
15 D. Azarifar and D. Sheikh, *Synth. Commun.*, 2013, **43**, 2517; F. Himo, Z. P. Demko, L. Noodleman and K. B. Sharpless, *J. Am. Chem. Soc.*, 2002, **124**, 12210.

16 V. Ponec and G. C. Bond, *Catalysis by Metals and Alloys*, Elsevier, Amsterdam, 1996.
17 C. W. Lim and I. S. Lee, *Nano Today*, 2010, **5**, 412.
18 D. Habibi, A. R. Faraji, M. Arshadi, S. Heydari and A. Gil, *Appl. Catal., A*, 2013, **466**, 282.
19 D. Habibi and A. R. Faraji, *Appl. Surf. Sci.*, 2013, **276**, 487.
20 W. Partenheimer, *Adv. Synth. Catal.*, 2004, **346**, 1495.
21 D. Habibi, A. R. Faraji, M. Arshadi, H. Veisi and A. Gil, *J. Mol. Catal. A: Chem.*, 2014, **382**, 41.
22 W. G. Finnegan, R. A. Henry and E. Lieber, *J. Org. Chem.*, 1953, **18**, 779.
23 R. A. Henry, W. G. Finnegan and E. Lieber, *J. Am. Chem. Soc.*, 1954, **76**, 88.
24 R. A. Henry, W. G. Finnegan and E. Lieber, *J. Am. Chem. Soc.*, 1955, **77**, 2264.
25 W. L. Garbrecht and R. M. Herbst, *J. Org. Chem.*, 1953, **18**, 1003.
26 W. L. Garbrecht and R. M. Herbst, *J. Org. Chem.*, 1953, **18**, 1022.
27 M. J. Frisch, W. W. Turcks, H. B. Schegel, G. E. S. Scuseria, M. A. Robb and J. R. Cheeseman, *Gaussian 03 revision B03*, Gaussian Inc., Pittsburgh, PA, 2003.
28 A. Frisch, A. B. Nielson and A. J. Holder, *Gaussview User Manual*, Gaussian Inc., Pittsburgh, PA, 2000.
29 L. Shiri, D. Sheikh, A. R. Faraji, M. Sheikhi and S. A. Seyed Katouli, *Lett. Org. Chem.*, 2014, **11**, 18.
30 K. Fukui, T. Yonezawa and H. J. Shingu, *J. Chem. Phys.*, 1952, **20**, 722.
31 Y. Li, Y. Liu, H. Wang, X. Xiong, P. Wei and F. Li, *Molecules*, 2013, **18**, 877.
32 E. Scrocco and J. Tomasi, *Adv. Quantum Chem.*, 1978, **11**, 115.
33 F. J. Luque, J. M. Lopez and M. Orozco, *Theor. Chem. Acc.*, 2000, **103**, 343.
34 N. Okulik and A. H. Jubert, *J. Mol. Des.*, 2005, **4**, 17.
35 P. Politzer and D. G. Truhlar, *Chemical Applications of Atomic and Molecular Electrostatic Potentials*, Plenum Press, New York, 1981.
36 K. C. D. Politzer, *The Force Concept in Chemistry*, Van Nostrand Reinhold Publisher, New York, 1981.
37 S. Ramachandran and G. Velraj, *Rom. J. Phys.*, 2013, **58**, 305.

